Water Research 215 (2022) 118249

Contents lists available at ScienceDirect

Water Research

journal homepage: www.elsevier.com/locate/watres

A semi-industrial scale AnMBR for municipal wastewater treatment at ambient temperature: performance of the biological process

Ángel Robles [a], Antonio Jiménez-Benítez [a,*], Juan Bautista Giménez [a], Freddy Durán [b], Josep Ribes [a], Joaquín Serralta [c], José Ferrer [c], Frank Rogalla [b], Aurora Seco [a]

[a] CALAGUA – Unidad Mixta UV-UPV, Departament d'Enginyeria Química, Universitat de València, Av. de la Universitat s/n, 46100 Burjassot, Valencia, Spain
[b] FCC Aqualia, S.A., Avenida Camino de Santiago, 40, 28050 Madrid, Spain
[c] CALAGUA – Unidad Mixta UV-UPV, Institut Universitari d'Investigació d'Enginyeria de l'Aigua i Medi Ambient – IIAMA, Universitat Politècnica de Valencia, Camí de Vera s/n, 46022 Valencia, Spain

ARTICLE INFO

Keywords:
Anaerobic membrane bioreactor (AnMBR)
Biological process
Demonstration plant
Methane production
Municipal wastewater (MWW)

ABSTRACT

A semi-industrial scale AnMBR plant was operated for more than 600 days to evaluate the long-term operation of this technology at ambient temperature (ranging from 10 to 27 °C), variable hydraulic retention times (HRT) (from 25 to 41 h) and influent loads (mostly between 15 and 45 kg COD·d^{-1}). The plant was fed with sulfate-rich high-loaded municipal wastewater from the pre-treatment of a full-scale WWTP. The results showed promising AnMBR performance as the core technology for wastewater treatment, obtaining an average 87.2 ± 6.1 % COD removal during long-term operation, with 40 % of the data over 90%. Five periods were considered to evaluate the effect of HRT, influent characteristics, COD/SO_4^{2-}-S ratio and temperature on the biological process. In the selected periods, methane yields varied from 70.2±36.0 to 169.0±95.1 STP L CH_4·kg^{-1} COD_{inf}, depending on the influent sulfate concentration, and wasting sludge production was reduced by between 8 % and 42 % compared to conventional activated sludge systems. The effluent exhibited a significant nutrient recovery potential. Temperature, HRT, SRT and influent COD/SO_4^{2-}-S ratio were corroborated as crucial parameters to consider in maximizing AnMBR performance.

1. Introduction

Anaerobic treatment of municipal wastewater (MWW) has several advantages over conventional aerobic processes, as has been widely recognized over the years. Its main advantages are: low sludge production due to low anaerobic biomass yield (Giménez et al., 2011); reduced energy consumption because no aeration is required (Lee et al., 2017); methane is produced from organic matter valorization, which improves the technology's energy balance (Krzeminski et al., 2017); low greenhouse gas emissions when methane is recovered from both biogas and effluent streams (Jiménez-Benítez et al., 2020b); and potential recovery potential of nutrients content (Batstone and Virdis, 2014). Moreover, the limitations associated with anaerobic processes applied to low-organic strength wastewaters (e.g. low growth rate of anaerobic biomass at ambient temperature or poor sludge settling properties) can be overcome by combining membrane technology and anaerobic reactors in the so-called anaerobic membrane bioreactor (AnMBR) (Ozgun et al., 2013), where the filtration process allows complete physical biomass retention. Hydraulic retention time (HRT) and sludge retention time (SRT) can thus be decoupled, which means high-rate reactors can be designed and high-quality effluent suitable for water reclamation can be achieved with the appropriate membrane pore-size (Jiménez-Benítez et al., 2020a). Eventually, membrane modules are more compact than the equivalent secondary settlers + disinfection units (e.g. UV process), which helps to reduce the layout footprint of wastewater treatment facilities and permits existing space-constrained treatment plants to be retrofitted (Xiao et al., 2019).

A high concentration of nutrients (mainly nitrogen and phosphorus,

Abbreviations: AnMR, anaerobic membrane bioreactor; BMP, biomethane potential; BOD_5, biological oxygen demand; CAS, conventional activated sludge; CE, circular economy; COD, chemical oxygen demand; GHG, greenhouse gas; HRT, hydraulic retention time; MA, methanogens; MWW, municipal wastewater; N, nitrogen; OLR, organic loading rate; P, phosphorus; SRB, sulfate-reducing bacteria; SRT, sludge retention time; STP, standard temperature and pressure; TSS, total suspended solids; VFA, volatile fatty acids; VSS, volatile suspended solids; WSP, waste-sludge production; WWTP, wastewater treatment plant; Y^{CH_4}, methane yield.

* Correspondence author
E-mail address: anluisji@uv.es (A. Jiménez-Benítez).

https://doi.org/10.1016/j.watres.2022.118249
Received 29 December 2021; Received in revised form 27 February 2022; Accepted 2 March 2022
Available online 4 March 2022

but also magnesium, potassium, etc.) in the effluent of anaerobic processes has traditionally been considered a significant environmental risk to aquatic ecosystems (eutrophication) and potable water resources when these streams are discharged (Pretel et al., 2016; Rodriguez-Garcia et al., 2011). This being true, it is also possible to consider it as an opportunity to introduce the fundamentals of the circular economy (CE) to wastewater treatment, since anaerobic treatments can be used to recover nutrients. Recovery plus recycling would contribute to closing both the materials and energy loops, and several processes and technologies are already available or being investigated to take advantage of these essential resources for agriculture and industry (Robles et al., 2020a). Including these resources in a comprehensive nutrient management system is becoming more important, as shown, among others, by the interest shown by the European Union in this matter (European Commission, 2015). At the present time, most efforts focus on the P since this element and phosphorite were included in European Critical Raw Materials lists in 2017 and 2014, respectively. However, N recovery is also attracting attention because of the high energy consumption and associated greenhouse gas emissions from its fixation from atmospheric N_2. Nutrient recovery thus helps to reduce both the dependence on their production and/or imports, which is even more important for those that are exhaustible such as phosphorus and potassium, and greenhouse gases (GHG) associated with mineral fertilizers, whose production results in significant energy expenditure (McCarty et al., 2011) and has an environmental impact.

Biosolids production has also been identified as a key issue in wastewater treatment; aerobic processes are characterized by high sludge production associated with a high biomass yield of aerobic metabolism, which involves a significant management cost that affects the economic and environmental performance of sewage treatments. Additionally, the regulation of waste sewage sludge, which is a challenge in wastewater treatment processes, is also expected to be tightened (Collivignarelli et al., 2019). AnMBR can help to overcome these problems in two ways: firstly, the anaerobic process mineralizes organic matter with reduced anabolism and low sludge production. By a way of example, Foladori et al. (2015) reported a sludge production in aerobic WWTPs of 0.25-0.35 kg VSS per kg COD removed (unstabilized sludge) and around 0.18 kg VSS per kg COD removed for stabilized sludge, respectively, while Robles et al. (2020) reported a stabilized sludge production in an AnMBR demonstration plant treating MWW of 0.148 kg VSS per kg COD removed. Secondly, biomass retention by membrane modules allows increasing SRT, which contributes to achieve on-site sludge stabilization and reduces or even avoids further sludge treatment.

A final consideration is that anaerobic removal of organic matter generates methane, a storable energy carrier suitable to produce renewable heat and power. Boosting anaerobic processes through AnMBR may thus improve the energy balance of existing wastewater treatment facilities. Using it as the core technology would take full advantage of the organic matter and the associated energy embedded in wastewater. At the same time, reduction of GHG emissions would be expected when grid energy consumption is replaced by energy recovery provided by this methane. However, despite these indisputable benefits, AnMBR technology presents three fundamental challenges: i) competition between sulfate-reducing bacteria (SRB) and methanogens (MA) for the same substrates reduces methane yields when treating influents with high sulfate contents (Durán et al., 2020); ii) reduction of sulfate by SRB produces sulfide and hydrogen sulfide, which eventually could entail inhibition in anaerobic metabolism and needs to be considered in energy recovery and water reclamation processes; and iii) dissolved methane losses through the effluent reduce energy recovery and, especially, increase GHG emissions (Jiménez-Benítez et al., 2020b). In this sense, co-digestion (e.g. the organic fraction of municipal waste, food waste, etc.) has been explored to increase influent organic load and thus increase methane production (Karki et al., 2021; Moñino et al., 2017), while several promising technologies for dissolved methane recovery (e.g. PDMS membranes) are also being studied (Sanchis-Perucho et al., 2020; Crone et al., 2016).

AnMBR technology is thus a clear candidate for renewing the wastewater treatment approach and would contribute to the economic, environmental and social goals of water management, with CE playing an active role. Persevering with a business-as-usual scenario based on conventional technologies, which have been shown to be effective but not efficient, would entail ignoring the current global context: climate change, energy transition, resource depletion, and environment degradation.

This work describes the results of operating of an AnMBR semi-industrial plant (demonstration scale, TRL of 6) for MWW treatment at the Alcázar de San Juan WWTP (Alcázar de San Juan, Ciudad Real, Spain). The size of the prototype, together with being fed with real MWW and operated for more than 2.5 years, means it can be considered a reliable and robust source of performance data. The main objective of the study was to contrast AnMBR with conventional wastewater treatments and demonstrate its potential benefits.

2. Materials and methods

2.1. AnMBR description and operation

Fig. 1 shows the process and instrumentation diagram (P&ID) of the semi-industrial AnMBR plant operated in this work. This plant mainly consists of a 40 m^3 (c.a. 34.4 m^3 working volume + 5.6 m^3 headspace) anaerobic reactor connected to three 0.8 m^3 membrane tanks (c.a. 0.7 m^3 working volume + 0.1 m^3 headspace). Each membrane tank was fitted with one ultrafiltration membrane system (PURON® PSH41, KMS, 0.03-μm pore size, total filtration area of 41 m^2), giving a total filtration area of 123 m^2. A sieve screw (RT, 1.5-mm screen size), an equalization tank (1.1 m^3) and a clean-in-place tank (0.37 m^3) were the other main elements in the plant. Total sludge volume was recorded considering the working volumes of both the anaerobic reactor and membrane tanks, accounting for 36.32±1.63 m^3 during the operating period. The AnMBR was equipped with a 2.1 m^2 degassing membrane unit for dissolved methane recovery, consisting of a polydimethylsiloxane (PDMS) hollow-fiber commercial module provided by PermSelect®, MedArray Inc. USA. The plant was fed with effluent from the pre-treatment step (sand and grease removal) of the Alcázar de San Juan WWTP (Alcázar de San Juan, Ciudad Real, Spain). Further details of this AnMBR system can be found in Robles et al. (2020).

Regarding filtration process, the system was able to operate with transmembrane flux in the range 14-21 LMH, with moderate sparging gas demand (11-14 $Nm^3_{biogas} \cdot m^{-3}_{permeate}$) and significant total suspended solids (TSS) (8-13 $g \cdot L^{-1}$). Transmembrane pressures varied between 87 and 490 mbar and fouling rates between 1.7 and 16.6 $mbar \cdot d^{-1}$. Only two chemical cleanings of membrane were needed during the considered experimental period.

The semi-industrial plant performance was assessed from two points of view: (i) considering the 610 days of operations included in this work; and (ii) selecting 5 periods from the overall operating period. It is important to highlight the variable influent quality and the relatively high COD and BOD concentrations due to the contributions of several nearby dairy and wine industries. During the operation period and based on data obtained in previous AnMBR pilot plant studies (Giménez et al., 2014, 2012; Seco et al., 2018), SRT was maintained at 70 days and the plant was operated at two different HRT (25-26 and 41 hours). Temperature varied freely between 10 and 27 °C (ambient temperature operation), while OLR was in the range between 0.60±0.20 and 1.28 ±0.38 kg $COD \cdot m^{-3} \cdot d^{-1}$. Table 1 shows the characterization of the influent and effluent streams together with the main operating conditions during the five selected periods.

2.2. AnMBR monitoring

The following parameters were regularly monitored in the influent:

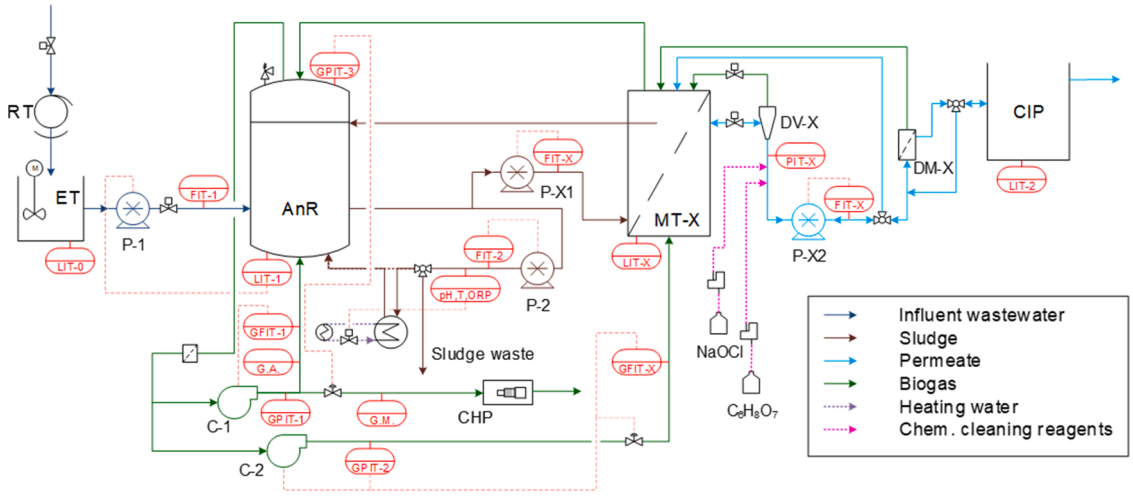

Fig. 1. Process and Instrumentation Diagram (P&ID).

Table 1
Influent and effluent characterization and operation conditions during the studied periods.

KEY REACTOR PARAMETERS	Units	I	II	III	IV	V
SRT	d	70±1	68±2	70±2	71±2	70±0
HRT	h	41±1	25±1	26±2	26±2	41±13
T	°C	27±1	24±2	19±1	27±1	18±2
INFLUENT	**Units**	**I**	**II**	**III**	**IV**	**V**
$Q_{treatment}$	$L{\cdot}d^{-1}$	21228±591	33016±2773	33243±3118	34207±1478	20984±7482
TSS	$mg{\cdot}L^{-1}$	462±188	418±293	332±145	354±116	430±120
VSS	%	64.6±5.9	82.0±11.5	63.1±14.6	75.5±9.6	80.1±13.0
COD	$mg{\cdot}L^{-1}$	1285±429	1403±532	896±201	755±224	1038±238
OLR	kg $COD{\cdot}m^{-3}{\cdot}d^{-1}$	0.75±0.25	1.28±0.38	0.82±0.19	0.71±0.23	0.60±0.20
BOD_5	$mg{\cdot}L^{-1}$	772±277	911±288	569±122	451±154	581±180
N_T	$mg\ N{\cdot}L^{-1}$	52.0±13.3	54.7±16.3	46.8±6.9	46.0±11.2	35.6±8.0
P_T	$mg\ P{\cdot}L^{-1}$	10.1±2.8	8.6±2.1	8.5±1.2	6.8±1.3	7.6±1.1
PO_4^{3-}-P	$mg\ P{\cdot}L^{-1}$	2.5±0.0	5.8±2.1	6.0±0.9	5.3±1.3	3.9±1.7
S^{2-}	$mg\ S{\cdot}L^{-1}$	37.9±26.7	59.6±19.5	47.0±38.7	30.7±49.2	38.3±14.5
SO_4^{2-}-S	$mg\ S{\cdot}L^{-1}$	147.7±13.3	172.2±28.5	125.4±47.6	157.3±46.9	149.7±26.9
$COD/\ SO_4^{2-}$-S	$g\ COD{\cdot}g^{-1}$-S	8.70±3.69	8.15±4.44	7.14±4.31	4.80±2.86	6.94±2.83
EFFLUENT	**Units**	**I**	**II**	**III**	**IV**	**V**
COD	$mg{\cdot}L^{-1}$	91±31	116±24	121±15	80±17	79±18
N_T	$mg\ N{\cdot}L^{-1}$	47.9±6.2	54.0±14.6	47.3±4.3	52.5±10.2	37.0±11.1
P_T	$mg\ P{\cdot}L^{-1}$	8.8±1.9	9.9±1.9	6.9±2.8	6.3±0.5	7.8±1.2
S^{2-}	$mg\ S{\cdot}L^{-1}$	174.3±28.7	207.5±73.2	233.1±66.3	183.2±27.0	166.2±27.9
VFA	$mg\ COD{\cdot}L^{-1}$	8.8±13.7	21.1±45.0	41.3±27.6	0.0±0.0	5.4±10.9
CH_4	$mg{\cdot}L^{-1}$	16.0±0.5	17.1±0.8	17.9±0.3	16.3±0.5	18.7±0.6
REACTOR	**Units**	**I**	**II**	**III**	**IV**	**V**
TSS	$g{\cdot}L^{-1}$	8.4±0.5	12.6±0.5	11.3±1.0	10.4±0.8	8.3±1.2
VSS	%	70.3±5.5	68.1±1.8	72.8±3.8	65.7±2.7	68.9±5.9
pH		7.1±0.1	7.0±0.1	7.0±0.1	7.0±0.1	7.0±0.3
Q_{WS}	$L{\cdot}d^{-1}$	522±5	511±107	521±5	510±18	520±4
COD	$g{\cdot}L^{-1}$	11.4±0.6	15.8±1.1	14.7±2.0	13.2±0.5	13.0±0.4
Q_{biogas}	$L\ STP{\cdot}d^{-1}$	5396±4435	5558±3204	1901±597	1359±999	2241±924
$\%CH_4$	%	77±2	77±2	72±2	77±2	76±1

total COD and BOD_5, sulfate (SO_4^{2-}-S), sulfide (HS^--S), total nitrogen (N_T), total phosphorus (P_T), nitrate (NO_3^--N), phosphate (PO_4^{3-}-P), TSS, and volatile suspended solids (VSS). Effluent characterization comprised total COD, N_T, P_T and HS-S, and volatile fatty acids (VFA). Finally, reactor monitoring was based on TSS, VSS, COD, pH, temperature and methane content in the biogas (% CH_4). Dissolved methane in the effluent was calculated by Henry's law and assuming saturation conditions. pH, temperature and biogas flow rate were registered online. 24-hour-composite samples were taken from the influent twice a week for all measurements except for COD, which was analyzed daily. Grab samples were taken twice a week from the effluent and mixed liquor.

2.3. Analytical methods

TSS, VSS, COD, BOD_5, sulfate, sulfide, and nutrients were determined according to Standard Methods (APHA, 2005). VFA concentration was determined by titration according to the method proposed by Moosbrugger et al. (1992).

2.4. Data processing and calculations

Different key performance indicators were calculated to evaluate the performance of the system as shown in Robles et al., (2020), *i.e.* methane

yield taking into account the methane dissolved in the permeate, COD removal rates, and biosolids production.

3. Results and discussion

The performance of the demonstration plant was evaluated for 610 days. Five periods were further characterized to assess the robustness of the AnMBR-technology against the disturbances in the main operating conditions derived from the natural variations throughout the year.

3.1. Organic removal efficiency

Fig. 2 shows the 15-day moving average for the influent organic load along with its 95% confidence bands, the daily average temperature, and both the removed and biodegraded COD. The influent organic load was highly variable, mainly due to the aforementioned variable industrial discharges. Biodegraded COD accounted for the COD that was biologically removed by SRB or was transformed into methane by MA, whereas the removed COD also considered the physically retained COD (by the ultrafiltration process) besides the biodegraded COD. Conversely, the influent sulfate-concentration variation was moderate, resulting in different COD/SO_4^{2-}-S ratios for each period (see Table 1). The temperature followed the natural variations in mid-latitude temperate climates, with strong variations between day to night (data not shown) and summer to winter. The daily-average temperature difference from winter to summer was higher than 17 °C.

The HRT was varied to simulate population shifts during summer and winter periods as a result of population density changes during vacation periods. Initially, HRT was set to 41 hours in period P1, in accordance with the low population-density in coastal areas before the summer. HRT was almost halved from P1 to P2 (25±1 h) and P4 (26±2 h) to simulate the intensification of water usage by the massive influx of tourists in coastal areas during vacation periods. Similarly, P3 y P5 were operated at the same low temperature (19±1 and 18±1 °C, respectively) but different HRT (25±1 h in P3 and 41±13 h in P5) to simulate population variation during the winter period. HRT was kept practically constant from period P2 to period P4 (around 25 h), representing densely populated all-year-long areas. However, as shown in Table 1, the OLR decreased (1.28±0.38 kg COD·m^{-3}·d^{-1} in P2, 0.82±0.19 kg COD·m^{-3}·d^{-1} in P3 and 0.71±0.23 kg COD·m^{-3}·d^{-1} in P4) as a result of the drop in the influent COD concentrations (1403±532 mg·L^{-1} in P2, 896±201 mg·L^{-1} in P3 and 755±224 mg·L^{-1} in P4), which was attributed to changes in the activity of the industries that discharge into the sewer system. The sulfate concentration also decreased from period P2 (172.2±28.5 mg S·L^{-1}) to period P3 (125.4±47.6 mg S·L^{-1}), albeit the COD reduction was more significant, resulting in a lower COD/SO_4^{2-}-S ratio. Conversely, the sulfate concentration in period P4 (157.3±46.9 mg S·L^{-1}) was higher than in period P3 despite the fact that COD concentration continued to fall, both contributing to a significant reduction in the COD/SO_4^{2-}-S ratio. SO_4^{2-}-S concentration in period P5 (149.7 ±26.9 mg S·L^{-1}) remaining similar to P4. The increased influent COD concentration in period P5 (1038±238 mg·L^{-1}) thus resulted in a higher COD/SO_4^{2-}-S ratio. Despite the higher COD concentration, OLR was lower in period P5 (0.60±0.20 kg COD·m^{-3}·d^{-1}) than in period P4 as a result of the higher HRT in period P5.

Fig. 2 shows that COD removal accounted for an average of 87.2 ± 6.1 % of the influent COD. 87 % of the COD removal data was higher than 80 %, whilst almost 40 % of the COD removal data was over 90 %. The membranes were able to virtually retain all particulates. However, the occasional unbalanced performance of the different stages in anaerobic degradation due to low temperatures or organic load peaks accumulated intermediate soluble organics that were able to pass through the membrane, thus increasing the effluent COD and reducing COD removal.

COD was not completely biodegraded by SRB or by MA. Conversely, a fraction of the removed COD was simply retained within the system due to membrane filtration, helping to increase the solids concentration and therefore waste-sludge production. Regarding the biologically removed COD, sulfate concentration was virtually zero in the effluent, indicating that SRB completely reduced influent sulfate (2 grams of COD were consumed per gram of SO_4^{2-}-S reduced). The analysis of the variance ANOVA of the COD consumed by SRB (expressed as OLR-SRB, i.e., the influent OLR which is consumed by SRB) found a significant difference between the mean values in the different periods (P-value = 0.0) (see complementary material). Nevertheless, Fischer's least significant difference (LSD) method for the pairwise comparison of mean values in the different periods were fairly similar in the mean values for the OLR-SRB among periods P1 and P5, and between periods P2 and P4. While P3 had an intermediate mean value.

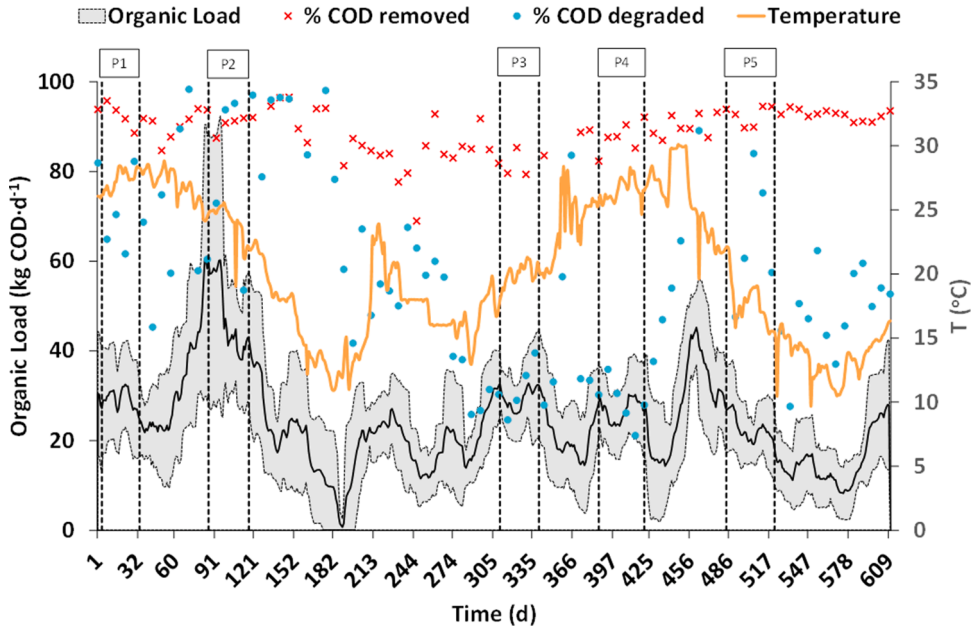

Fig. 2. Operating conditions during the experimental period.

The remaining COD was theoretically available for MA (i.e., OLR-MA) in the proportion shown in Fig. 3. As can be seen in this figure, the OLR in period P2 was much higher than the others, as a result of the strengthened influent wastewater organic load. During P2, 24.5 % of the OLR was consumed by SBR (OLR-SBR) while 75.5 % remained available for MA (OLR-MA). On the other hand, P4 showed the lowest OLR-MA (58.3 %). The P-value for the analysis of the variance of the OLR-MA (see complementary material) in each period was lower than 0.05 (P-value = 0.0) again indicating a significant difference between the mean values in the different periods. In this case, Fischer's LSD method found significant similarity between mean values of P1 and P3, and between P4 and P5. P2 had the highest mean value for OLR available for MA due to the high treatment flow and influent COD concentration.

The system's response to organic-load peaks entailed an accumulation of VFA, likely due to the faster response of acid-generating than acid-consuming organisms, although the system was able quickly restore the equilibrium. The VFA effluent concentrations were low in the periods with longer HRT (P1 and P5) and moderate organic overloads. Also, higher operating temperatures were associated with lower VFA concentrations (P1, P2 and P4). In contrast, the combination of short HRT and lower temperature of P3 led to more severe organic overloading and hindered accumulated VFA consumption, resulting in the highest VFA effluent concentrations (see Table 1). This result is attributed to the more severe impairment of acid consuming organisms, which seemed to be more affected by lower temperatures than acid-producing organisms.

3.2. Methane production

Table 2 shows the percentages of the COD removed by filtration and biodegradation and biodegraded COD. As aforementioned, the COD removed was higher in periods P1 (93.1±6.3 %) and P5 (92.5±3.5 %), when HRT was higher (41±1 and 41±13 h, respectively), indicating that the extended contact time between soluble organics and anaerobic microorganisms enabled MA to further consume the organic matter and produce CH_4 and CO_2. The absence of intermediate products indicates that the intermediate anaerobic degradation steps were properly balanced, hydrolysis and solubilization being the limiting steps.

The percentage of biodegraded COD in P1 and P2 was higher than the rest of the periods (71.3±27.7 % and 74.4±14.5 %, respectively) due to their high influent COD concentration (1285±429 mg COD·L^{-1} in P1 and 1403±532 mg COD·L^{-1} in P2) and temperature (27±1 °C and 24±2 °C, respectively), which favored bacterial metabolism and hence organic matter consumption. P4, with 63.4±26.2 % of biodegraded COD, also presents a high operating temperature (27±1 °C) but, also the lowest influent COD concentration (755±224 mg COD·L^{-1}). The percentage of biodegraded COD in P4 is similar to those obtained in P3 (61.0±16.2 %) and P5 (61.4±13.0 %), operated at low temperatures (18±2 °C and 19 ±1 °C, respectively), but with higher influent COD (896±201 mg COD·L^{-1} in P3 and 1038±238 mg COD·L^{-1} in P5).

Fig. 4 depicts the time evolution of the 15-day moving average biogas production along with its 95 % confidence bands. As can be seen, the biogas production trend was directly related to the fraction of COD load available for MA (OL-MA), although it was also influenced by temperature, which limited the production of substrates for SRB and MA as a result of the reduction in the hydrolysis and solubilization rates.

The capacity of the system to recover energy was evaluated in terms of methane yield (Y^{CH_4}), which stands for the amount of methane produced per unit of influent COD. The biomethane potential (BMP) representing the fraction of the influent COD that ended up as methane (by comparing Y^{CH_4} to the theoretical maximal methane production, i.e., 350 STP L CH_4·kg^{-1} COD) was also calculated. The resulting Y^{CH_4} and BMP in the different periods are shown in Table 2. However, only the results regarding Y^{CH_4} will be discussed, since the BMP results followed the same trend.

The highest Y^{CH_4} value was obtained in P1 (169.0±95.1 STP L CH_4·kg^{-1} COD) with a combination of high T (27±1 °C) and HRT (41±1 h). Its influent COD/SO_4^{2-}-S ratio was also the most favorable for methane production (8.70±3.69 COD·g^{-1} SO_4^{2-}-S). While a high temperature enhanced the hydrolysis rate, which is considered the limiting stage in anaerobic digestion, methane production increased with the COD available for MA, for which P1 had the highest percentage of influent COD available for MA (77.0 %, see Fig. 3). In contrast, the slight temperature drop and reduced HRT reduction between periods P1 and P2 (24±2 °C and 25±1 h, respectively) helped to reduce the Y^{CH_4} to 109.6±70.0 STP L CH_4·kg^{-1} COD, even when Fischer's LSD method showed that the amount of COD for MA in P2 was the highest (35 kg·d^{-1}). It is important to highlight that an error of 18.5 % was obtained when COD mass balance was applied to P2 (see Fig. 5 and discussed in section 3.5). This COD loss could be attributed to underestimated biogas production. As mentioned above, dissolved methane in the effluent was

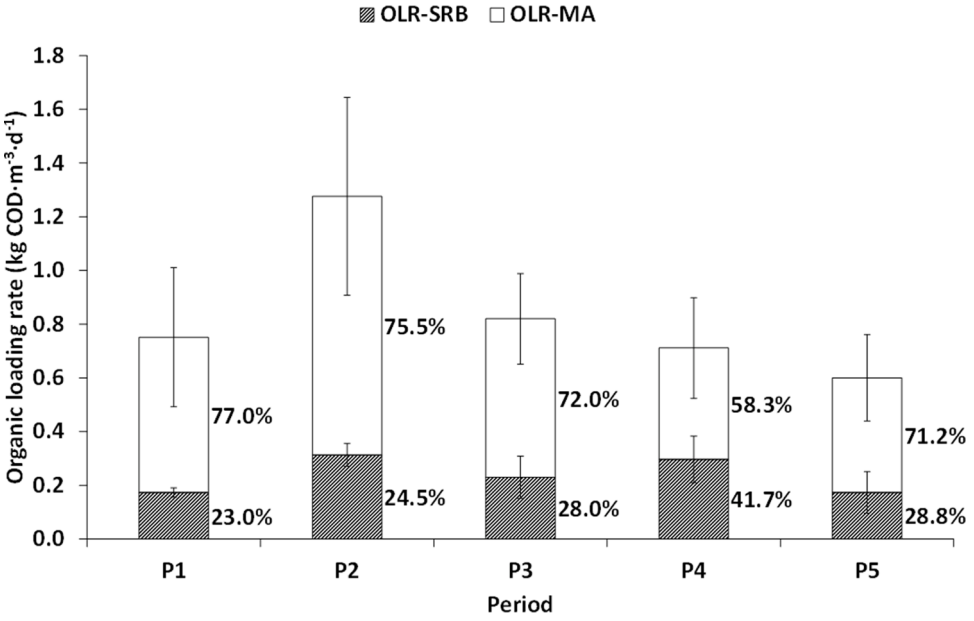

Fig. 3. Organic loading rate consumed by SRB and available for MA.

Table 2
Percentage of COD removed and biodegraded, methane yield (Y^{CH_4}), biomethane potential (BMP) per influent COD and waste sludge production (WSP) per kg of influent and removed COD.

Period	SRT (d) Mean ±SD	HRT (h) Mean ±SD	T (°C) Mean ±SD	COD_{rem} (%) Mean ±SD	$COD_{biodegraded}$ (%) Mean±SD	(STP L $CH_4 \cdot kg^{-1}$ COD) Mean±SD	BMP (%) Mean±SD	WSP (kg VSS·kg^{-1} COD_{inf}) Mean±SD	WSP (kg VSS·kg^{-1} COD_{rem}) Mean±SD
P1	70±1	41±1	27±1	93.1±6.3	71.3±27.7	169.0±95.1	48.3 ±28.3	0.112±0.045	0.121±0.067
P2	68±2	25±1	24±2	91.9±2.7	74.4±14.5	109.6±70.0	31.3 ±22.1	0.095±0.032	0.103±0.044
P3	70±2	26±2	19±1	86.7±4.7	61.0±16.2	75.2±16.9	21.5±4.8	0.144±0.050	0.166±0.074
P4	71±2	26±2	27±1	89.5±4.9	63.4±26.2	70.2±36.0	20.1 ±10.8	0.135±0.055	0.150±0.079
P5	70±0	41±13	18±2	92.5±3.5	61.4±13.0	102.3±63.8	29.2 ±18.2	0.137±0.061	0.148±0.072

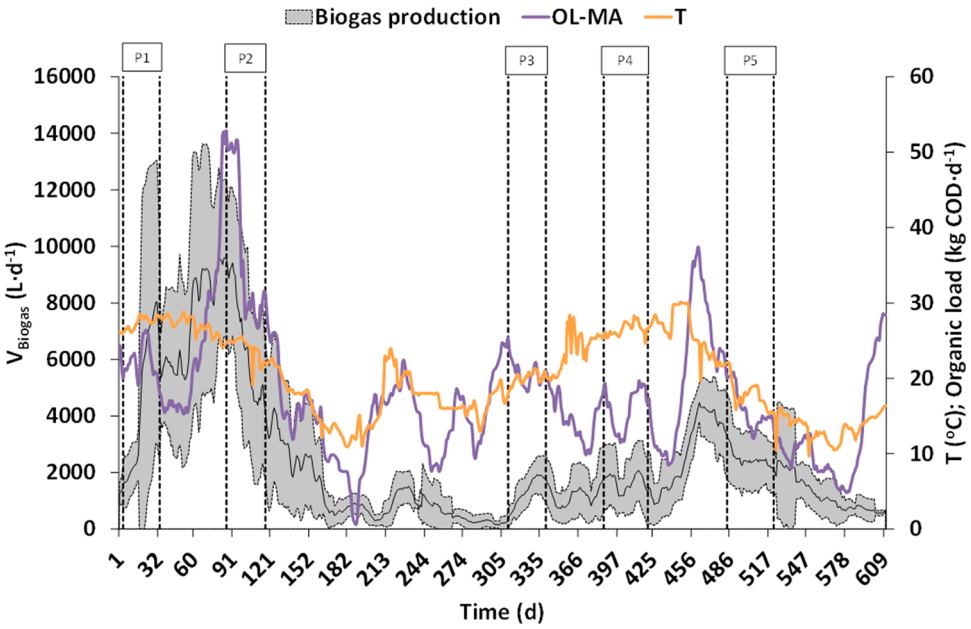

Fig. 4. Time evolution of the biogas production trend, temperature and organic load available for MA.

calculated assuming saturation conditions, although there could have been oversaturation episodes (Pauss et al., 1990).

P3 and P4 present the lowest Y^{CH_4} values (75.2±16.9 and 70.2±36.0 STP L $CH_4 \cdot kg^{-1}$ COD, respectively). These results can also be explained by the temperature, HRT and COD/SO_4^{2-}-S ratio. Despite P3 being operated with a moderate influent COD/SO_4^{2-}-S ratio (7.14±4.31 g COD·g^{-1} SO_4^{2-}-S) and available organic matter (72.0 %), influent COD could not offset its low operating temperature (19±1 °C) and HRT (26±2 h), which hindered hydrolysis and possibly also methane production. In P4, the operating temperature was favorable (27±1 °C) and HRT remained at 26±2 h, but the COD/SO_4^{2-}-S ratio was significantly lower than in the other periods (4.80±2.86 g COD·g^{-1} SO_4^{2-}-S), which justifies the lower Y^{CH_4}.

Finally, similar Y^{CH_4} values were obtained for P2 and P5 (109.6 ±70.0 and 102.3±63.8 STP L $CH_4 \cdot kg^{-1}$ COD, respectively). In this case, P2 had high temperature (24±2 °C) and high COD/SO_4^{2-}-S ratio (8.15 ±4.44 g COD·g^{-1} SO_4^{2-}-S) but lower HRT (25±1 h). P5 operated at high HRT (41±13 h), a moderate influent COD/SO_4^{2-}-S ratio (6.94±2.83 g COD·g^{-1} SO_4^{2-}-S) but the lowest temperature (18±2 °C). Considering that influent quality cannot be modified, HRT thus becomes the main design parameter for maximizing methane production in low winter temperatures.

It should be remembered that influent sulfate concentration depends on the region in which the wastewater is generated, since it is associated with the concentration of sulfate in water sources as well as the possible contribution of factories that discharge sulfur to the sewage system. Since the COD consumed by SRB is biodegradable and should have undergone at least the first stages of anaerobic degradation (i.e., hydrolysis and solubilization) to be available for SRB, it would also have been available for MA. A sulfate-free influent would thus have yielded a much higher Y^{CH_4} and BMP would have been similar to the percentage of biodegraded COD. As way of example, methane yields without considering the COD consumed by SRB in the studied periods, $Y_{SO_4}^{CH_4}$, would rise to 87.4-191.0 STP L $CH_4 \cdot kg^{-1}$ COD. However, in sulphate-rich wastewater, the role of SRB in reducing the effluent-soluble COD when HRT is reduced must be considered, since SRB has higher degradation rates than MA, especially at lower temperatures.

3.3. Biosolids

The waste-sludge production (WSP) expressed in kg VSS per kg of influent COD and per kg of removed COD is shown in Table 2. The reported values are the outcome of a complex interaction between operational conditions and influent characteristics. The fraction and

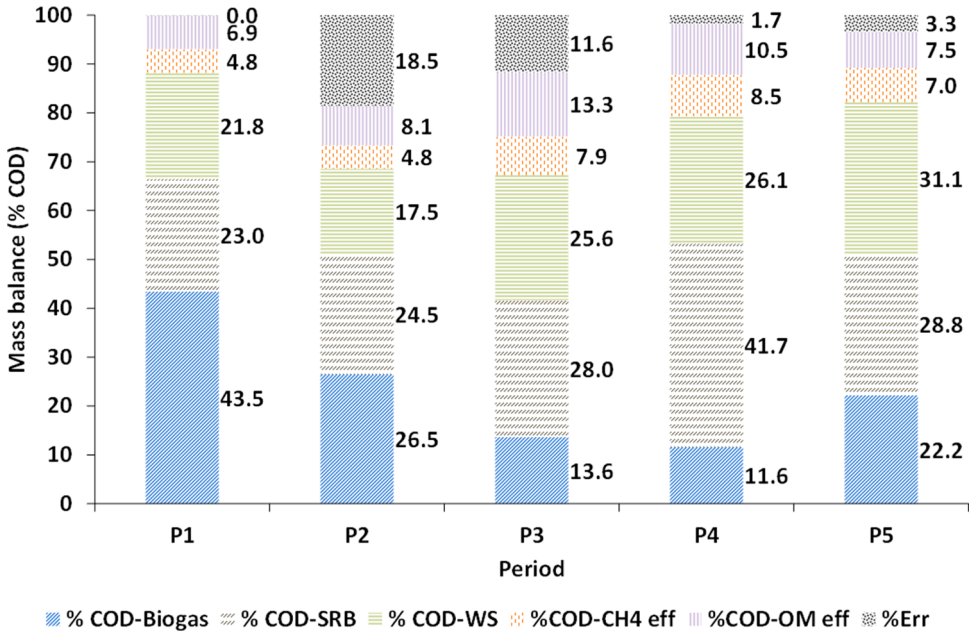

Fig. 5. COD mass balance.

composition of particulates in the influent and their fate within the system, which depends on the operating conditions (temperature, HRT and especially SRT), influence the accumulation and retention of biosolids and therefore increased WSP. A greater influx of solids into the system entails greater accumulation and retention unless the operating conditions favor hydrolysis and solubilization. On the other hand hydrolysis is widely accepted as the limiting step in anaerobic degradation and is severely affected by temperature drops (Batstone, 2006). Although temperature also affects the following steps of the anaerobic degradation, results indicated that intermediates accumulation can be mitigated as long as HRT is high enough. In the same way, WSP can also be reduced by increasing system SRT, thus extending the time for further hydrolysis and solubilization of the accumulated solids.

As can be seen in Table 2, P3 had the highest WSP (0.166±0.074 kg VSS·kg^{-1} COD$_{rem}$) mainly due to the low temperature (19±1 °C). The operating conditions hindered biodegradability and therefore raised sludge production. P4 and P5 also had high WSP (0.150±0.079 kg VSS·kg^{-1} COD$_{rem}$ and 0.148±0.072 kg VSS·kg^{-1} COD$_{rem}$, respectively) although lower than P1. The high production in P5 can be attributed to the lowest operating temperature (18±2 °C). However, despite temperature in P4 being the highest (27±1 °C) the significant WSP in this period was associated with its low COD/SO_4^{2-}-S (4.80±2.86 g COD·g^{-1} SO_4^{2-}-S). In this period, the percentage of influent COD consumed by SRB accounted for 41.7 % while in the other periods was below 29 %. Since the SRB biomass yield was significantly higher than MA, the associated solids production was also higher, as was sludge production in this period (Durán et al., 2020).

Finally, P1 and P2 had the lowest WSP (0.121±0.067 and 0.103 ±0.044 kg VSS·kg^{-1} COD$_{rem}$, respectively). Both were operated at high temperature (27±1 °C in P1 and 24±2 °C in P2) and had the highest COD/SO_4^{2-}-S ratio (8.70±3.69 g COD·g^{-1} SO_4^{2-}-S and 8.15±4.44 g COD·g^{-1} SO_4^{2-}-S, respectively). The combination of both variables enhanced MA organic matter biodegradation and reduced sludge production. P2 was also characterized by the highest percentage of influent VSS, COD and BOD_5, indicating the highest influent wastewater biodegradability and that the operating conditions were appropriate for the maximum biosolids degradation. It is important to highlight that, besides the complex interaction of factors that affect the WSP, it can be as low as 0.103±0.044 kg VSS·kg^{-1} COD$_{rem}$.

As a way of comparison, Foladori et al., (2015) reported 0.23-0.35 kg VSS·kg^{-1} COD$_{rem}$ (SRT of around 10-20 days) and 0.18 kg VSS·kg^{-1} COD$_{rem}$ for aerobic treatment without and with sludge stabilization, respectively. According to these values, all the selected periods had lower WSP than the aerobic treatments with percentage reductions between 8 % (P3) and 43 % (P2). Increasing SRT over 70 days could be expected to lead to lower WSP and additional biosolids stabilization, although solids concentration in the reactor would also rise and affect processes such as membrane filtration in the operating stage or increase reactor capacities' requirements in the design stage. In this regard, Ji et al., (2020) obtained a WSP of 0.09 kg VSS·kg^{-1} COD$_{rem}$ operating two different AnMBR with different pore size membranes for 120 days at 25°C. In this work no excess sludge was wasted during long-term operations except for the sludge samples. This value confirms that it is possible to achieve low WSP with high SRTs. On the other hand, with the same technology Seco et al., (2018) reported a WSP of 0.218 kg VSS·kg^{-1} COD$_{rem}$ with an SRT of 140 days and 27°C. Design and operating conditions thus need to be carefully selected taking influent characteristics into account and especially the particulate COD and COD/SO_4^{2-}-S ratio.

3.4. Nutrients recovery potential

Anaerobic treatments have low nutrients requirements per COD removed, as can be seen from the effluent characterization shown in Table 1, which confirms that AnMBR is promising technology for turning wastewater into a source of nutrients. N_T and P_T concentrations in the effluent accounted for 37.0-54.0 mgN·L^{-1} and 6.3-9.9 mgP·L^{-1}, respectively. Considering the treatment capacity of "Alcázar de San Juan" WWTP (16000 m^3·d^{-1}), these concentrations represent 216 – 315 t N·year^{-1} and 37 – 58 t P·year^{-1}. It should be noted that over 90 % of European phosphorus applications are import-dependent, so that wastewater can play an active role as a P supplier by combining AnMBR and CE fundamentals (Rosemarin et al., 2020). Selecting urea ($CO(NH_2)_2$) and P_2O_5 as representative N-based and P-based fertilizers, respectively, nutrients equivalent to 463-676 t Urea·year^{-1} and 84-132 t P_2O_5·year^{-1} could be provided by effluent. If a price of €273.6 per t of urea (bib31) and €783.0 per t of P_2O_5 (bib30) is assumed, the mineral-fertilizer equivalent-value of the nutrients in the discharge flow would be between k€162 and k€230 per year, and would pay for 10-15%

of water treatment costs at €0.269 per m^3 for AnMBR (Jiménez-Benítez et al., 2020a).

To reduce production costs and impact, an alternative embedded nutrient strategy consists of direct reuse (fertigation) instead of producing fertilizers from effluent, which makes AnMBR technology especially suitable for decentralized plants in rural areas where the effluent can be discharged directly to farmland. It is important to highlight that apart from a nutrient-rich stream the combination of an anaerobic process with UF membrane implemented in an AnMBR produces an effluent free of solids and pathogens (Krzeminski et al., 2017), which makes it especially appropriate for fertigation. For example, "Alcázar de San Juan" WWTP could cover an annual winter wheat crop (productivity 6.7 t grain·ha^{-1}) of 1080-1575 ha attending to N needs (0.2 t·ha^{-1}) and 1527-2400 ha if P_2O_5 requirements are considered (0.055 t·ha^{-1}) (Roy et al., 2006).

3.5. COD mass balance and overall performance considerations

Fig. 5 shows the COD mass balance in the periods studied. Each sector of the circles depicts the fraction of the influent COD (i.e., COD biodegraded by SRB, COD associated with biogas, COD from dissolved methane, COD wasted with sludge, COD in the effluent and mass balance error).

P1 shows no mass balance error but periods P2 to P5 have positive values in all cases indicating that the influent COD is higher than COD leaving the system through biogas, effluent, wasted sludge and COD biodegraded by SRB. The errors in P4 (1.7 %) and P5 (3.3 %) are negligible, while P2 and P3 show significant errors (18.5 % and 11.6 %, respectively). As all the parameters involved in COD mass balance (e.g., flow rates, COD concentration, biogas production, waste sludge, etc.) are based on analytical and/or on-line measurements except for dissolved methane (calculated as stated in Section 2.2), it is hypothesized that in these two periods dissolved methane in the effluent have been underestimated. As mentioned above, dissolved methane is calculated considering saturation conditions based on Henry's law, although oversaturation could take place in these periods due to methane bubbles passing through the membranes or poor reactor mixing.

Fig. 5 confirms the influence of operating at high T, HRT and COD/SO_4^{2-}-S ratio to enhance methane production, with P1, P2 and P5 showing the highest percentages of biogas associated to COD. P1, operated at the highest temperature, HRT and COD/SO_4^{2-}-S ratio (27±1 °C, 41±1 h and 8.70±3.69 g COD·g^{-1} SO_4^{2-}-S, respectively), shows a percentage of 43.5 % of biogas-associated COD, the highest value. P2 was operated at high temperature (24±2 °C) and a favorable COD/SO_4^{2-}-S ratio (8.15±4.44 g COD·g^{-1} S). Both conditions could offset the lower HRT (25±1 h) and kept biogas production at significant percentages (26.5 %). If the COD mass balance error (18.5 %) is attributed to underestimated methane production, the biogas percentage could rise to 45 %, as in P1. P5 also presented significant biogas production (22.2 %). This period operated at high HRT (41±1 h) and moderate influent COD/SO_4^{2-}-S ratio (6.94±2.83 g COD·g^{-1} SO_4^{2-}-S), but the lowest T (18 ±2 °C), which hindered methane production. Since a negligible error was obtained for this period, potential increased biogas production due to underestimated dissolved methane cannot be considered.

The lowest percentages of COD associated with biogas were obtained in P3 (13.6 %) and P4 (11.6 %). P3 operated at a low temperature (19±1 °C) and HRT (26±2 h) and therefore with low biogas production despite a favorable influent COD/SO_4^{2-}-S ratio (7.14±4.31 g COD·g^{-1} SO_4^{2-}-S), similar to P5. However, if mass balance error is considered (11.6 %), biogas-associated COD could rise to 25.2 %. P4, with low HRT (26±2 h) and the lowest influent COD/SO_4^{2-}-S ratio (4.80±2.86 g COD·g^{-1} SO_4^{2-}-S) had the lowest COD percentage associated with methane production (11.6 %), despite its favorable operating temperature (27±1 °C).

For the COD associated with waste sludge, Fig. 5 shows that P5 had the highest percentage (31.1 %). This period operated at the lowest T (18±2 °C), which hindered particulate degradation, and the lowest OLR (0.60±0.20 kg COD·m^{-3}·d^{-1}). Since OLR before P5 was higher than in this period (see Fig. 2), the sludge wasted during P5 could have been influenced by accumulated VSS. P2 had a percentage of 17.2 %, due to its favorable operating temperature (24±2 °C) and the highest OLR (1.28±0.38 kg COD·m^{-3}·d^{-1}). P3 and P4 show a similar percentage associated with waste sludge (25.6 % and 26.1 %, respectively), despite operating at very different temperatures (19±1 °C in P3 and 27±1 in P4 °C). This can be attributed to the higher COD percentage consumed by SRB (41.7 %) in P4. As these bacteria have a higher growth yield than MA and therefore increase solids production in the reactor.

The results show an overall promising performance of AnMBR technology for treating MWW at ambient temperature. The COD removal capacity allows compliance with treatment regulation (e.g., MWWTD); methane yields indicate its potential for organic matter valorization and energy recovery; and nutrient content in the effluent indicates its capacity for turning wastewater into a valuable source of nutrients. Low waste-sludge production means AnMBR can be considered a robust candidate as the new core technology to boost the transition of wastewater treatment plants towards the new resource recovery facilities, especially suitable for small and decentralized plants in which anaerobic processes are not currently applied.

Temperature, HRT, SRT and COD/SO_4^{2-}-S ratio are crucial parameters to improve technological, economic and environmental performance of AnMBR technology for wastewater treatment, HRT and SRT being the only ones which do not depend on ambient conditions. Both HRT and SRT thus appear as the main design parameter. It is important to highlight the benefits that the implementation and optimization of dissolved methane recovery technologies (e.g., hollow-fiber membranes) can provide to AnMBR: dissolved methane will improve the wastewater treatment energy balances while the carbon footprint associated with greenhouse gas emissions is minimized.

4. Conclusions

An industrial AnMBR prototype was operated for 610 days during which an average of 87.2 ± 6.1 % of influent COD removal was achieved, with 87 % of the data over 80 % and almost 40 % over 90 %. UF membranes contributed to wastewater treatment by retaining almost all the particulates. In addition, in the long-term operations, 5 periods were selected to evaluate the performance of the AnMBR. In these periods, a Y^{CH_4} between 70.2 and 169.0 STP L CH_4·kg^{-1} COD were achieved and methane percentages in the biogas varied from 75 to 77 %. Sludge production ranged between 0.103±0.044 and 0.166±0.074 kg VSS·kg^{-1} COD_{rem}, which represents a reduction of 9 to 43 % compared to CAS. A significant nutrient recovery potential was also identified.

Finally, temperature, HRT and COD/SO_4^{2-}-S ratio jointly with SRT are crucial parameters to take into account in maximizing AnMBR's technical, economic and environmental performance. However, since temperature and influent COD/SO_4^{2-}-S depend on ambient conditions, HRT could be considered the main design parameter jointly with SRT.

Declaration of Competing Interest

None.

Acknowledgement

The authors are grateful to the European Commission for the co-financing of the LIFE MEMORY project (LIFE13 ENV/ES/ 001353) and the staff of Aguas de Alcázar for their close collaboration.

Supplementary materials

Supplementary material associated with this article can be found, in the online version, at doi:10.1016/j.watres.2022.118249.

References

APHA, 2005. Standard Methods for the Examination of Water and Wastewater. American Public Health Association, Washington, DC.

Batstone, D.J., 2006. Mathematical modelling of anaerobic reactors treating domestic wastewater: Rational criteria for model use. Rev. Environ. Sci. Biotechnol. 5, 57–71. https://doi.org/10.1007/s11157-005-7191-z.

Batstone, D.J., Virdis, B., 2014. The role of anaerobic digestion in the emerging energy economy. Curr. Opin. Biotechnol. 27, 142–149. https://doi.org/10.1016/J.COPBIO.2014.01.013.

Collivignarelli, M.C., Abbà, A., Miino, M.C., Torretta, V., 2019. What advanced treatments can be used to minimize the production of sewage sludge in WWTPs? Appl. Sci. 9 https://doi.org/10.3390/app9132650.

Crone, B.C., Garland, J.L., Sorial, G.A., Vane, L.M., 2016. Significance of dissolved methane in effluents of anaerobically treated low strength wastewater and potential for recovery as an energy product: A review. Water Res 104, 520–531. https://doi.org/10.1016/J.WATRES.2016.08.019.

Durán, F., Robles, A., Giménez, J.B., Ferrer, J., Ribes, J., Serralta, J., 2020. Modeling the anaerobic treatment of sulfate-rich urban wastewater: Application to AnMBR technology. Water Res 11133. https://doi.org/10.1016/j.watres.2020.116133.

Commission, European, 2015. Communication from the Commission to the European Parliament, the Council, the European Economic and Social Committee and the Committee of the Regions. Closing the loop - An EU action plan for the Circular Economy. Official Journal of the European Union.

Foladori, P., Andreottola, G., Ziglio, G., 2015. Sludge Reduction Technologies in Wastewater Treatment Plants. Sludge Reduction Technologies in Wastewater Treatment Plants. https://doi.org/10.2166/9781780401706.

Giménez, J.B., Martí, N., Ferrer, J., Seco, A., 2012. Methane recovery efficiency in a submerged anaerobic membrane bioreactor (SAnMBR) treating sulphate-rich urban wastewater: Evaluation of methane losses with the effluent. Bioresour. Technol. 118, 67–72. https://doi.org/10.1016/j.biortech.2012.05.019.

Giménez, J.B., Martí, N., Robles, A., Ferrer, J., Seco, A., 2014. Anaerobic treatment of urban wastewater in membrane bioreactors: Evaluation of seasonal temperature variations. Water Sci. Technol. 69, 1581–1588. https://doi.org/10.2166/wst.2014.069.

Giménez, J.B., Robles, A., Carretero, L., Durán, F., Ruano, M.V., Gatti, M.N., Ribes, J., Ferrer, J., Seco, A., 2011. Experimental study of the anaerobic urban wastewater treatment in a submerged hollow-fibre membrane bioreactor at pilot scale. Bioresour. Technol. 102, 8799–8806. https://doi.org/10.1016/J.BIORTECH.2011.07.014.

Ji, J., Sakuma, S., Ni, J., Chen, Y., Hu, Y., Ohtsu, A., Chen, R., Cheng, H., Qin, Y., Hojo, T., Kubota, K., Li, Y.Y., 2020. Application of two anaerobic membrane bioreactors with different pore size membranes for municipal wastewater treatment. Sci. Total Environ. 745, 140903 https://doi.org/10.1016/j.scitotenv.2020.140903.

Jiménez-Benítez, A., Ferrer, F.J., Greses, S., Ruiz-Martínez, A., Fatone, F., Eusebi, A.L., Mondéjar, N., Ferrer, J., Seco, A., 2020a. AnMBR, reclaimed water and fertigation: Two case studies in Italy and Spain to assess economic and technological feasibility and CO2 emissions within the EU Innovation Deal initiative. J. Clean. Prod. 270, 122398 https://doi.org/10.1016/j.jclepro.2020.122398.

Jiménez-Benítez, A., Ferrer, J., Rogalla, F., Vázquez, J.R., Seco, A., Robles, Á., Mannina, G., Pandey, A., Larroche, C., Ng, H.Y., 2020b. 12 - Energy and environmental impact of an anaerobic membrane bioreactor (AnMBR) demonstration plant treating urban wastewater. In: Ngo, H.H.B.T. (Ed.), Current Developments in Biotechnology and Bioengineering. Elsevier, pp. 289–310. https://doi.org/10.1016/B978-0-12-819854-4.00012-5.

Karki, R., Chuenchart, W., Surendra, K.C., Shrestha, S., Raskin, L., Sung, S., Hashimoto, A., Kumar Khanal, S., 2021. Anaerobic co-digestion: Current status and perspectives. Bioresour. Technol. 330, 125001 https://doi.org/10.1016/j.biortech.2021.125001.

Krzeminski, P., Leverette, L., Malamis, S., Katsou, E., 2017. Membrane bioreactors – A review on recent developments in energy reduction, fouling control, novel configurations, LCA and market prospects. J. Memb. Sci. 527, 207–227. https://doi.org/10.1016/j.memsci.2016.12.010.

Lee, M., Keller, A.A., Chiang, P.-C., Den, W., Wang, H., Hou, C.-H., Wu, J., Wang, X., Yan, J., 2017. Water-energy nexus for urban water systems: A comparative review on energy intensity and environmental impacts in relation to global water risks. Appl. Energy 205, 589–601. https://doi.org/10.1016/J.APENERGY.2017.08.002.

McCarty, P.L., Bae, J., Kim, J., 2011. Domestic Wastewater Treatment as a Net Energy Producer–Can This be Achieved? Environ. Sci. Technol. 45, 7100–7106. https://doi.org/10.1021/es2014264.

Moñino, P., Aguado, D., Barat, R., Jiménez, E., Giménez, J.B., Seco, A., Ferrer, J., 2017. A new strategy to maximize organic matter valorization in municipalities: Combination of urban wastewater with kitchen food waste and its treatment with AnMBR technology. Waste Manag 62, 274–289. https://doi.org/10.1016/j.wasman.2017.02.006.

Moosbrugger, R.E., Wentzel, M.C., Ekama, G.A., Marais, G., 1992. **Simple titration procedures to determine H2CO3* alkalinity and short-chain fatty acids in aqueous solutions**. Pretoria.

Ozgun, H., Dereli, R.K., Ersahin, M.E., Kinaci, C., Spanjers, H., Van Lier, J.B., 2013. A review of anaerobic membrane bioreactors for municipal wastewater treatment: Integration options, limitations and expectations. Sep. Purif. Technol. 118, 89–104. https://doi.org/10.1016/j.seppur.2013.06.036.

Pauss, A., Andre, G., Perrier, M., Guiot, S.R., 1990. Liquid-to-Gas mass transfer in anaerobic processes: Inevitable transfer limitations of methane and hydrogen in the biomethanation process. Appl. Environ. Microbiol. 56, 1636–1644. https://doi.org/10.1128/aem.56.6.1636-1644.1990.

Pretel, R., Robles, A., Ruano, M.V., Seco, A., Ferrer, J., 2016. Economic and environmental sustainability of submerged anaerobic MBR-based (AnMBR-based) technology as compared to aerobic-based technologies for moderate-/high-loaded urban wastewater treatment. J. Environ. Manage. 166 https://doi.org/10.1016/j.jenvman.2015.10.004.

Robles, Á., Aguado, D., Barat, R., Borrás, L., Bouzas, A., Giménez, J.B., Martí, N., Ribes, J., Ruano, M.V., Serralta, J., Ferrer, J., Seco, A., 2020a. New frontiers from removal to recycling of nitrogen and phosphorus from wastewater in the Circular Economy. Bioresour. Technol. https://doi.org/10.1016/j.biortech.2019.122673.

Robles, Á., Durán, F., Bautista, J., Jiménez, E., Ribes, J., Serralta, J., Seco, A., Ferrer, J., Rogalla, F., 2020b. Anaerobic membrane bioreactors (AnMBR) treating urban wastewater in mild climates. Bioresour. Technol. 314, 123763 https://doi.org/10.1016/j.biortech.2020.123763.

Rodriguez-Garcia, G., Molinos-Senante, M., Hospido, A., Hernández-Sancho, F., Moreira, M.T., Feijoo, G., 2011. Environmental and economic profile of six typologies of wastewater treatment plants. Water Res 45, 5997–6010. https://doi.org/10.1016/j.watres.2011.08.053.

Rosemarin, A., Macura, B., Carolus, J., Barquet, K., Ek, F., Järnberg, L., Lorick, D., Johannesdottir, S., Pedersen, S.M., Koskiaho, J., Haddaway, N.R., Okruszko, T., 2020. Circular nutrient solutions for agriculture and wastewater – a review of technologies and practices. Curr. Opin. Environ. Sustain. 45, 78–91. https://doi.org/10.1016/j.cosust.2020.09.007.

Roy, R., Finck, a, Blair, G., Tandon, H., 2006. Nutrient management guidelines for some major field crops. Plant Nutr. food Secur 235–348.

Seco, A., Mateo, O., Zamorano-López, N., Sanchis-Perucho, P., Serralta, J., Martí, N., Borrás, L., Ferrer, J., 2018. Exploring the limits of anaerobic biodegradability of urban wastewater by AnMBR technology. Environ. Sci. Water Res. Technol. 4, 1877–1887. https://doi.org/10.1039/c8ew00313k.

www.echemi.com, 2022. www.echemi.com [WWW Document]. URL. https://www.echemi.com/productsInformation/pd20150901061-phosphoric-acid.html.

www.indexmundi.com, 2022. www.indexmundi.com [WWW Document]. URL. https://www.indexmundi.com/commodities/?commodity=urea.

Xiao, K., Liang, S., Wang, X., Chen, C., Huang, X., 2019. Current state and challenges of full-scale membrane bioreactor applications: A critical review. Bioresour. Technol. 271, 473–481. https://doi.org/10.1016/J.BIORTECH.2018.09.061.